RNA polymerase errors cause splicing defects and can be regulated by differential expression of RNA polymerase subunits.

Lucas B. Carey[1*]

[1] Department of Experimental and Health Sciences, Universitat Pompeu Fabra, Dr. Aiguader 88, 08003 Barcelona, Spain.

[*] Correspondence to: Lucas B. Carey (lucas.carey@upf.edu)

Errors during transcription may play an important role in determining cellular phenotypes: the RNA polymerase error rate is >4 orders of magnitude higher than that of DNA polymerase and errors are amplified >1000-fold due to translation. However, current methods to measure RNA polymerase fidelity are low-throughout, technically challenging, and organism specific. Here I show that changes in RNA polymerase fidelity can be measured using standard RNA sequencing protocols. I find that RNA polymerase is error-prone, and these errors can result in splicing defects. Furthermore, I find that differential expression of RNA polymerase subunits causes changes in RNA polymerase fidelity, and that coding sequences may have evolved to minimize the effect of these errors. These results suggest that errors caused by RNA polymerase may be a major source of stochastic variability at the level of single cells.

24 The information that determines protein sequence is stored in the genome
25 but that information must be transcribed by RNA polymerase and translated by the
26 ribosome before reaching its final form. DNA polymerase error rates have been well
27 characterized in a variety of species and environmental conditions, and are low, on
28 the order of one mutation per 10^8 - 10^{10} bases per generation[1-3]. In contrast, RNA
29 polymerase errors are uniquely positioned to generate phenotypic diversity. Error
30 rates are high (10^{-6}-10^{-5})[4-7], and each mRNA molecule is translated into 2,000 –
31 4,000 molecules of protein[8,9], resulting in amplification of any errors. Likewise,
32 because many RNAs are present in less than one molecule per cell in microbes[10,11]
33 and embryonic stem cells[12], an RNA with an error may be the only RNA for that
34 gene; all newly translated protein will contain this error. Despite the fact that
35 transient errors can result in altered phenotypes[13,14], the genetics and
36 environmental factors that affect RNA polymerase fidelity are poorly understood.
37 This is because current methods for measuring polymerase fidelity are technically
38 challenging[4], require specialized organism-specific genetic constructs[15], and can
39 only measure error rates at specific loci[16].
40
41 To overcome these obstacles I developed MORPhEUS (Measurement Of RNA
42 Polymerase Errors Using Sequencing), which enables measurement of differential
43 RNA polymerase fidelity using existing RNA-seq data **(Figure 1)**. The input is a set
44 of RNA-seq fastq files and a reference genome, and the output is the error rate at
45 each position in the genome. I find that RNA polymerase errors result in intron
46 retention and that cellular mRNA quality control may reduce the effective RNA

47 polymerase error rate. Moreover, our analyses suggest that the expression level of
48 the RPB9 Pol II subunit determines RNA polymerase fidelity *in-vivo*. Because it can
49 be run on any existing RNA-seq data, MORPhEUS enables the exploration of a
50 previously unexplored source of biological diversity in microbes and mammals.
51
52 Technical errors from reverse transcription and sequencing, and biological
53 errors from RNA polymerase look identical (single-nucleotide differences from the
54 reference genome). Therefore, a major challenge in identifying SNPs and in
55 measuring changes in polymerase fidelity is the reduction of technical errors[17-
56 19]**(Figure 1)**. First, I map full length (untrimmed) reads to the genome, and discard
57 reads with indels, more than two mismatches, reads that map to multiple locations
58 in the genome, and reads that do not map end-to-end along the full length of the
59 read. I next trim the ends of the mapped reads, as alignments are of lower quality
60 along the ends, and the mismatch rate is higher, especially at splice junctions. I also
61 discard any cycles within the run with abnormally high error rates, and bases with
62 low Illumina quality scores **(Figure 1 – figure supplement 1)**. Finally, using the
63 remaining bases, I count the number of matches and mismatches to the reference
64 genome at each position in the genome. I discard positions with identical
65 mismatches that are present more than once, as these are likely due to subclonal
66 DNA polymorphisms or sequences that Illumina miscalls in a systematic manner[20]
67 **(Figure 1 – figure supplement 2)**. The result is a set of mismatches, many of which
68 are technical errors, some of which are RNA polymerase errors. In order to
69 determine if RNA-seq mismatches are due to RNA polymerase errors it is necessary

70 to identify sequence locations in which RNA polymerase errors are expected to have
71 a measurable effect, or situations in which RNA polymerase fidelity is expected to
72 vary.
73
74 I reasoned that RNA polymerase errors that alter positions necessary for
75 splicing should result in intron retention, while sequencing errors should not affect
76 the final structure of the mRNA **(Figure 2a)**. However, mutations in the donor and
77 acceptor splice sites also result in decreased expression[36], and therefore are difficult
78 to measure using RNA-seq. I therefore used chromatin-associated and nuclear RNA
79 from Hela and Huh7 cells[37], and extracted all reads that span an exon-intron
80 junction for introns with canonical GT and AG splice sites, and measured the RNA-
81 seq mismatch rate at each position. I find that errors at the G and U in the 5' donor
82 site, and at the A in the acceptor site are significantly enriched relative to errors at
83 other positions **(Figure 2b)**, and to errors trinucleotides present in the splicing
84 motifs in the human genome **(Figure 2 – figure supplement 1)** suggesting that
85 RNA polymerase mismatches can result in changes in transcript isoforms. The
86 ability of RNA polymerase errors to significantly affect splicing has been proposed[22]
87 but never previously measured.
88
89 RPB9 is known to be involved in RNA polymerase fidelity *in vitro* and *in*
90 *vivo*[15,23]. I therefore reasoned that cell lines expressing low levels of RPB9 would
91 have higher RNA polymerase error rates. Consistent with this, I find that RPB9
92 expression varies 8-fold across the ENCODE cell lines, and this expression variation

93 is correlated with the RNA-seq error rate **(Figure 2c, Figure 2 – figure supplement**
94 **2)**. This suggests that low RPB9 expression may cause decreased polymerase
95 fidelity *in-vivo*.
96
97 In addition, export of mRNAs from the nucleus involves a quality-control
98 mechanism that checks if mRNAs are fully spliced and have properly formed 5' and
99 3' ends[24]. I hypothesized that mRNA export may involve a quality control that
100 removes mRNAs with errors. I used the ENCODE dataset in which nuclear and
101 cytoplasmic poly-A+ mRNAs I re sequenced, thus I can compare nuclear and
102 cytoplasmic fractions from the same cell line grown in the same conditions and
103 processed in the same manner. I find that the nuclear fraction has a higher RNA
104 polymerase error rate than does the cytoplasmic fraction **(Figure 2c,d)**, suggesting
105 that either that nuclear RNA-seq has a higher technical error rate or that the cell has
106 mechanisms for reducing the effective polymerase error rate by preventing the
107 export of mRNAs that contain errors.
108
109 Rpb9 and Dst1 are known to be involved in RNA polymerase fidelity *in-vitro*,
110 yet there is conflicting evidence as to the role of Dst1 *in-vivo*[6,15,23,25-27]. Part of these
111 conflicts may result from the fact that the only available assays for RNA polymerase
112 fidelity are special reporter strains that rely on DNA sequences known to increase
113 the frequency of RNA polymerase errors. While I found that RPB9 expression
114 correlates with RNA-seq error rates in mammalian cells, correlation is not
115 causation. Furthermore, differences in RNA levels do not necessitate differences in

116 stoichiometry among the subunits in active Pol II complexes. In order to determine
117 if differential expression of RPB9 or DST1 are causative for differences in RNA
118 polymerase fidelity in-vivo, I constructed two yeast strains in which I can alter the
119 expression of either RPB9 or DST1 using B-estradiol and a synthetic transcription
120 factor that has no effect on growth rate or the expression of any other genes[28,29]. I
121 grew these two strains (Z_3EV_{pr}-RPB9 and Z_3EV_{pr}-DST1) in different concentrations
122 of B-estradiol and performed RNA-seq. I find that cells expressing low levels of
123 RPB9 have high RNA polymerase error rates **(Figure 3a)**. Likewise, cells with low
124 DST1 have high error rates **(Figure 3a)**. The increase in errors rate is not a property
125 of cells defective for transcription elongation **(Figure 3 – figure supplement 1)**.
126 The increase in error rates due to mutations in Rpb9 and Dst1 have not been
127 robustly measured, however, there are some rough numbers. Here, the measured
128 increase in error rate is 13%, while the measured effect of Rpb9 deletion *in*-vitro is
129 5-fold[38] and in-vivo following reverse transcription is 30%[25]. If 2% of the observed
130 mismatches are due to RNA polymerase errors, a 5-fold increase in polymerase
131 error rate results in a 10% increase in measured mismatch frequency; this is
132 consistent with RNA polymerase fidelity of 10^{-6}-10^{-5} and overall RNA-seq error rates
133 of 10^{-4}. Note that in our assay cells still express low levels or RPB9, and we therefore
134 expect the increase in error rate to be lower, suggesting that RNA polymerase errors
135 constitute 5-10% of the measured mismatches. Our ability to genetically control the
136 expression of DST1 and RPB9, and measure changes in RNA-seq error rates is
137 consistent with MORPhEUS measuring RNA polymerase fidelity. In addition, we
138 observe more single nucleotide insertions in the RNA-seq data from the high error

139 rate samples, suggestiong that depletion of RPB9 and DST1 results in increased
140 insertions in transcripts, but not increased deletions **(Figure 3 – figure**
141 **supplement 2)**. Finally, genetic reduction in RNA polymerase fidelity results in
142 increased intron retention, consistent with RNA polymerase errors causing reduced
143 splicing efficiency **(Figure 3b)**.
144
145 A unique advantage of MORPhEUS is that it measures thousands of RNA
146 polymerase errors across the entire transcriptome in a single experiment, and thus
147 enables a complete characterization of the mutation spectrum and biases of RNA
148 polymerase. I asked how altered RPB9 and DST1 expression levels affect each type
149 of single nucleotide change. I find that, with decreasing polymerase fidelity,
150 transitions increase more than transversions, and that C->U errors are the most
151 common **(Figure 3c)**. This result, along with other sequencing based results[4], have
152 shown that DNA and RNA polymerase have broadly similar error profiles[2]; it will be
153 interesting to see if all polymerases share the same mutation spectra, and if this is
154 due to deamination of the template base, or is a structural property of the
155 polymerase itself. Interestingly, I find that coding sequences have evolved so that
156 errors are less likely to produce in-frame stop codons than out-of-frame stop
157 codons, suggesting that natural selection may act to minimize the effect of
158 polymerase errors **(Figure 4)**.
159
160 Here I have presented proof that relative changes in RNA polymerase error
161 rates can be measured using standard Illumina RNA-seq data. Consistent with

162 previous work *in-vivo* and *in-vitro*, I find that depletion of RPB9 or Dst1 results in
163 higher RNA polymerase error rates. Futhermore, I find that expression of RPB9
164 negatively correlates with RNA-seq error rates in human cell lines, suggesting that
165 differential expression of RPB9 may regulate RNA polymerase fidelity in-vivo in
166 humans. In addition, consistent with the errors detected by MORPhEUS being due to
167 RNA polymerase and not technical errors, in reads spanning an exon-intron
168 junction, the measured error rate is higher at the 5' donor splice site, suggesting that
169 RNA polymerase errors result in intron retention. Because it can be run on existing
170 RNA-seq data, I expect MORPhEUS to enable many future discoveries regarding both
171 the molecular determinants of RNA polymerase error rates, and the relationship
172 between RNA polymerase fidelity and phenotype.
173

174 ## Acknowledgements

175 I thank members of the Carey lab and the computational genomics groups in the
176 PRBB for thoughtful discussions.
177

178 ## Materials and methods

179 ### Counting RNA polymerase errors in already aligned ENCODE data

180 Much existing RNA-seq data is available as bam files aligned to the human
181 genome. In order to bypass the most computationally expensive step of the pipeline,

182 I developed a method capable of using RNA-seq reads aligned with spliced aligners.
183 First, in order to avoid increased mismatch rates at splice junctions due to
184 alignment problems with both spliced and unspliced reads, I used samtools[30] and
185 awk to remove all alignments that don't align along the full length of the genome
186 (eg: for 76bp reads, only reads with a CIGAR flag of 76M). The remaining reads I re
187 trimmed (bamUtil , trimBam) to convert the first and last 10bp of each read to Ns
188 and set the quality strings to '!'. I then used samtools mpileup (-q30 –C50 –Q30) and
189 custom perl code to count the number of reads and number of errors at each
190 position in genome. Positions with too many errors (eg: more than one read of the
191 same non-reference base) I re not counted.
192

193 ## Measurement of error rates at splice junctions

194 I used the UCSC table browser[31] to download two bed files: hg19
195 EnsemblGenes introns with -10bp flanking from each side, and another file with the
196 introns and +10bp flanking on either side. I then used bedtools[32] (bedtools flank -b
197 20 -l 0 & bedtools flank -l 20 -b 0) to generate bed files with intervals that contain
198 the splicing donor and acceptor sites, respectively. In addition, I used bedtools
199 getfasta on the +10bp flanking bed file to keep only introns flanked by GT and AG
200 donor and acceptor sites. The final result is a pair of bam files with intervals
201 centered on the splicing donor or acceptor sites. I used this new bed file to count
202 error rates around each splice junction. The error rate at each position (eg: -10, -9, -
203 8, etc from the G at the 5' donor site) is the sum of all errors at that position, divided
204 by the sum of all reads. Positions are relative to the splicing feature, not to the

205 genome, as error rates at any single genomic position are dominated by sampling
206 bias. Per mono, di and tri-nucleotide background error rates I re calculated using
207 the same scripts, but without limiting mpileup to the splice junctions.
208

209 ## Strain construction and RNA sequencing for RPB9 and DST1 strains

210 The parental strain DBY12394[33] (GAL2+ s288c repaired HAP1, ura3Δ,
211 leu2Δ0::ACT1pr-Z3EV-NatMX) was transformed with a PCR product (KanMX-
212 Z3EVpr) to generate a genomically integrated inducible RPB9 (LCY143) or DST1
213 (LCY142). Correct transformants I re confirmed by PCR. To induce various levels of
214 expression, strains I re grown in YPD + 0,3,6,12 or 25nM β-estradiol (Sigma E4389)
215 for more than 12 hours to a final OD_{600} of 0.1 – 0.4. Cellular RNA was extracted using
216 the Epicenter MasterPure RNA Purification Kit, and Illumina sequencing libraries I
217 re prepared using the Truseq Stranded mRNA kit, and sequenced on a HiSeq2000
218 with at least 20,000,000 50bp sequencing reads per sample.
219

220 I used bwa[34] (-n 2, to permit no more than two mismatches in a read) to align the
221 yeast RNA-seq reads to the reference genome, and trimBam from bamUtil to mask
222 the first and last 10bp of each read. I used samtools mpileup[30] (-q 30 -d 100000 -
223 C50 –Q39) to count the number of reads and mismatches at each position in the
224 genome, discarding low confidence mapping, reads that map to multiple positions,
225 and low quality reads. Duplicate reads can be removed from the fastq file if the
226 coverage is low enough so that all unique read sequences are expected to come the

227 same RNA fragment; this is the case for low coverage paired-end reads with a
228 variable insert size, but not for very high coverage datasets or single-ended reads.
229

230 **pre-existing RNA-seq datasets.**

231 For the intron retention analysis in human cells, data are from NCBI SRA
232 PRJNA253670. Data for the elc4 and spt4 analysis are from PRJNA167772 and
233 PRJNA148851, respectively. For RPB9 correlation, ENCODE[35] data (SRA
234 PRJNA30709) are all from the Gingeras lab at CSHL.

235 Competing financial interests

236 The author declares no competing financial interests.

237 References

238 1. Lynch, M. The lower bound to the evolution of mutation rates. *Genome Biol*
239 *Evol* **3,** 1107–1118 (2011).
240 2. Zhu, Y. O., Siegal, M. L., Hall, D. W. & Petrov, D. A. Precise estimates of mutation
241 rate and spectrum in yeast. *PNAS* **111,** E2310–8 (2014).
242 3. Lang, G. I. & Murray, A. W. Estimating the per-base-pair mutation rate in the
243 yeast Saccharomyces cerevisiae. *Genetics* **178,** 67–82 (2008).
244 4. Gout, J.-F., Thomas, W. K., Smith, Z., Okamoto, K. & Lynch, M. Large-scale
245 detection of in vivo transcription errors. *PNAS* **110,** 18584–18589 (2013).
246 5. Lynch, M. Evolution of the mutation rate. *Trends Genet.* **26,** 345–352 (2010).

247 6. Shaw, R. J., Bonawitz, N. D. & Reines, D. Use of an in vivo reporter assay to test
248 for transcriptional and translational fidelity in yeast. *J. Biol. Chem.* **277,**
249 24420–24426 (2002).
250 7. de Mercoyrol, L., Corda, Y., Job, C. & Job, D. Accuracy of wheat-germ RNA
251 polymerase II. General enzymatic properties and effect of template
252 conformational transition from right-handed B-DNA to left-handed Z-DNA.
253 *Eur. J. Biochem.* **206,** 49–58 (1992).
254 8. Schwanhäusser, B. *et al.* Global quantification of mammalian gene expression
255 control. *Nature* **473,** 337–342 (2011).
256 9. Futcher, B., Latter, G. I., Monardo, P., McLaughlin, C. S. & Garrels, J. I. A
257 sampling of the yeast proteome. *Mol. Cell. Biol.* **19,** 7357–7368 (1999).
258 10. Fuhrmann, C. N., Halme, D. G., O'Sullivan, P. S. & Lindstaedt, B. A complete set
259 of nascent transcription rates for yeast genes. *PLoS ONE* **5,** e15442–249
260 (2010).
261 11. Hereford, L. M. & Rosbash, M. Number and distribution of polyadenylated
262 RNA sequences in yeast. *Cell* **10,** 453–462 (1977).
263 12. Islam, S. *et al.* Characterization of the single-cell transcriptional landscape by
264 highly multiplex RNA-seq. *Genome Res.* **21,** 1160–1167 (2011).
265 13. Gordon, A. J. E., Satory, D., Halliday, J. A. & Herman, C. Heritable change caused
266 by transient transcription errors. *PLoS Genet.* **9,** e1003595–e1003595 (2013).
267 14. Gordon, A. J., Satory, D., Halliday, J. A. & Herman, C. Lost in transcription:
268 transient errors in information transfer. *Curr. Opin. Microbiol.* **24C,** 80–87
269 (2015).

270 15. Irvin, J. D. *et al.* A genetic assay for transcription errors reveals multilayer
271 control of RNA polymerase II fidelity. *PLoS Genet.* **10,** e1004532 (2014).
272 16. Imashimizu, M., Oshima, T., Lubkowska, L. & Kashlev, M. Direct assessment of
273 transcription fidelity by high-resolution RNA sequencing. *Nucleic Acids Res.*
274 **41,** 9090–9104 (2013).
275 17. Kleinman, C. L. & Majewski, J. Comment on "Widespread RNA and DNA
276 sequence differences in the human transcriptome". *Science* **335,** 1302–author
277 reply 1302 (2012).
278 18. Pickrell, J. K., Gilad, Y. & Pritchard, J. K. Comment on "Widespread RNA and
279 DNA sequence differences in the human transcriptome". *Science* **335,** 1302–
280 author reply 1302 (2012).
281 19. Li, M. *et al.* Widespread RNA and DNA sequence differences in the human
282 transcriptome. *Science* **333,** 53–58 (2011).
283 20. Meacham, F. *et al.* Identification and correction of systematic error in high-
284 throughput sequence data. *BMC Bioinformatics* **12,** 451 (2011).
285 21. Tilgner, H. *et al.* Deep sequencing of subcellular RNA fractions shows splicing
286 to be predominantly co-transcriptional in the human genome but inefficient
287 for lncRNAs. *Genome Res.* **22,** 1616–1625 (2012).
288 22. Fox-Walsh, K. L. & Hertel, K. J. Splice-site pairing is an intrinsically high fidelity
289 process. *Proc. Natl. Acad. Sci. U.S.A.* **106,** 1766–1771 (2009).
290 23. Knippa, K. & Peterson, D. O. Fidelity of RNA polymerase II transcription: Role
291 of RPB9 in error detection and proofreading. *Biochemistry* **52,** 7807–7817
292 (2013).

293 24. Lykke-Andersen, J. mRNA quality control: Marking the message for life or
294 death. *Curr. Biol.* **11,** R88–91 (2001).
295 25. Nesser, N. K., Peterson, D. O. & Hawley, D. K. RNA polymerase II subunit Rpb9
296 is important for transcriptional fidelity in vivo. *Proc. Natl. Acad. Sci. U.S.A.* **103,**
297 3268–3273 (2006).
298 26. Walmacq, C. *et al.* Rpb9 Subunit Controls Transcription Fidelity by Delaying
299 NTP Sequestration in RNA Polymerase II. *J. Biol. Chem.* **284,** 19601–19612
300 (2009).
301 27. Kireeva, M. L. *et al.* Transient reversal of RNA polymerase II active site closing
302 controls fidelity of transcription elongation. *Mol. Cell* **30,** 557–566 (2008).
303 28. McIsaac, R. S., Gibney, P. A., Chandran, S. S., Benjamin, K. R. & Botstein, D.
304 Synthetic biology tools for programming gene expression without nutritional
305 perturbations in Saccharomyces cerevisiae. *Nucleic Acids Res.* **42,** e48–e48
306 (2014).
307 29. McIsaac, R. S., Oakes, B. L., Botstein, D. & Noyes, M. B. Rapid synthesis and
308 screening of chemically activated transcription factors with GFP-based
309 reporters. *Journal of visualized experiments : JoVE* e51153–e51153 (2013).
310 30. Li, H. *et al.* The Sequence Alignment/Map format and SAMtools. *Bioinformatics*
311 **25,** 2078–2079 (2009).
312 31. Karolchik, D. *et al.* The UCSC Table Browser data retrieval tool. *Nucleic Acids*
313 *Res.* **32,** D493–6 (2004).
314 32. Quinlan, A. R. & Hall, I. M. BEDTools: a flexible suite of utilities for comparing
315 genomic features. *Bioinformatics* **26,** 841–842 (2010).

316 33. McIsaac, R. S. *et al.* Synthetic gene expression perturbation systems with
317 rapid, tunable, single-gene specificity in yeast. *Nucleic Acids Res.* **41,** e57–e57
318 (2013).
319 34. Li, H. & Durbin, R. Fast and accurate short read alignment with Burrows-
320 Wheeler transform. *Bioinformatics* **25,** 1754–1760 (2009).
321 35. ENCODE Project Consortium. An integrated encyclopedia of DNA elements in
322 the human genome. *Nature* **489,** 57–74 (2012).
323 36 Jung, H. et al. Intron retention is a widespread mechanism of tumor-
324 suppressor inactivation. Nat. Genet. (2015).
325 37. Dhir, A. *et al.* Microprocessor mediates transcriptional termination of long
326 noncoding RNA transcripts hosting microRNAs. Nat. Struct. Mol. Biol. 22, 319–
327 327 (2015).
328 38. Walmacq, C. et al. Rpb9 subunit controls transcription fidelity by delaying
329 NTP sequestration in RNA polymerase II. J. Biol. Chem. 284, 19601–19612
330 (2009).
331
332
333

334 ## Figures

335 **Figure 1. A computational framework to measure relative changes in RNA**
336 **polymerase fidelity. (a)** Pipeline to identify potential RNA polymerase errors in
337 RNA-seq data. High quality full-length RNA-seq reads are mapped to the reference
338 genome or transcriptome using bwa, and only reads that map completely with two
339 or fewer mismatches are kept. **(b)** Then 10bp from the front and 10bp from the end
340 of the read are discarded as these regions have high error rates and are prone to
341 poor quality local alignments. **(c)** Errors that occur multiple times (purple boxes)
342 are discarded, as these are likely due to sub-clonal DNA mutations or sequences that
343 sequence poorly on the HiSeq. Unique errors in the middle of reads (cyan box) are
344 kept and counted.
345
346
347 **Figure 2. RNA polymerase errors cause intron retention and error rates are**
348 **correlated with RPB9 expression. (a)** RNA polymerse errors at the splice junction
349 should result in intron retention, as DNA mutations at the 5' donor site are known to
350 cause intron retention. **(b)** Shown are the RNA-seq mismatch rates at each position
351 relative to the 5' donor splice site, for sequencing reads that span an exon-intron
352 junction. Mismatch rates from chromatin associated and nuclear RNAs are higher at
353 the 5' and 3' splice sites, suggesting that RNA polymerase errors at this site result in
354 intron retention. **(c)** For all ENCODE cell lines, RPB9 expression was determined
355 from whole-cell RNA-seq data, and the RNA-seq error rate was measured separately
356 for the cytoplasmic and nuclear fractions. **(d)** The RNA-seq error rate is higher

357 (paired t-test, p=0.0019) in the nuclear than the cytoplasmic fraction, suggesting
358 that quality control mechanism may block nuclear export of low quality mRNAs.
359 **Figure 3. RNA polymerase error rate is determined by the expression level of**
360 **RPB9 and DST1. (a)** RNA-seq error rates I re measured for two strains (Z_3EVpr-
361 RPB9, black points , Z_3EVpr-DST1, blue points) grown at different concentrations of
362 β-estradiol. The points show the relationship between RPB9 expression levels
363 (determined by RNA-seq) and RNA-seq error rates. The blue points show RPB9
364 expression levels for the Z_3EVpr-DST1 strain, in which DST1 expression ranges from
365 16 FPKM at 0nM β-estradiol to 120 FPKM native expression to 756 FPKM at 25nM
366 β-estradiol. Low induction of both DST1 or RPB9 results in high RNA-seq error rates
367 (red box), while wild-type and higher induction levels result low RNA-seq error
368 rates (black box). **(b)** Across all genes, the intron retention rate is higher in
369 conditions with low RNA polymerase fidelity (t-test between high and low error rate
370 samples, p=0.029), consistent with the hypothesis that RNA polymerase errors
371 result in splicing defects. **(c)** The error rate for each of the 12 single base changes
372 are shown for induction experiments that gave high (red) or low (black) RNA-seq
373 error rates. Transitions (G<->A , C<->U) are marked with green boxes and
374 transversions (A<->C , G<->U) with purple
375
376 **Figure 4. In-frame stop codons are less likely to be created by polymerase**
377 **errors.** For all genes in yeast, I calculated the number of codons which are one
378 polymerase error from a stop codon. **(a)** Fewer in-frame codons can be turned into a
379 stop codon by a single nucleotide change, compared to out-of-frame codons. **(b)**

380 Codons that are one error away from generating an in-frame stop codon are more
381 likely to be found at the ends of ORFs, compared to the beginning of the ORF.
382
383 **Figure 1 – figure supplement 1. Cycle-specific error rates and better**
384 **differentiation of genetically determined error rates using base quality value**
385 **cutoffs.** Six yeast RNA-cDNA libraries were sequenced on the same lane in a HiSeq.
386 **(a)** The average mismatch rate (across the six cDNA libraries) to the reference
387 genome at each position was determined using different minimum base-quality
388 thresholds using GATK ErrorRatePerCycle. Independent of the quality threshold,
389 cycles at the ends, as well as some cycles in the middle, have high error rates. **(b)**
390 The measured error rate for each sample using a minimum base quality of 10. **(c)**
391 The measured error rate for each sample using a minimum base quality of 39.
392
393 **Figure 1 – figure supplement 2. RNA-seq data are enriched for mismatches to**
394 **the reference genome that occur far more often than expected.**
395 **(a)** At each coverage (x-axis), a point is shown if there is any positions in the
396 genome with the observed number of errors (y-axis) (small black dots). The
397 diagonal lines show mismatch frequencies of 100%, 10%, 1% and 0.1% — any point
398 falling on these lines has the given mismatch frequency. With large grey circles are
399 shown simulated data in which the same coverage as the yeast RNA-seq data are
400 used, but with a mismatch frequency identical to the measured overall mismatch
401 frequency of the yeast data. Locations in the graph in which a black point occurs but
402 there is no grey point are locations in which there are more mismatches than

403 expected by change. Note that at a coverage of less than 100, we expect to see no
404 mismatches more than twice, and 0.5% of positions with 2 observances of identical
405 mismatches. **(b)** Identical to (a) but with the simulated mismatch frequency 5x the
406 observed. **(c)** Shown are measured mismatch frequencies for the yeast RPB9 and
407 DST1 induction data at different B-estradiol concentrations, at different filters for
408 the maximal allowed number of observed identical mismatches. The dashed lines
409 show the average mismatch frequency for the 0nM condition. For all filters, low B-
410 estradiol conditions have higher RNA-seq mismatch frequencies. **(d)** The coverage
411 of the yeast RNA-seq data; ~95% of the genome is covered by less than 100 reads.
412 **(e)** Shown are the fraction of positions in the genome (y-axis) with X errors (x-axis)
413 for the yeast RNAseq data (cyan) and simulated data (blue). Also shown are the
414 same data for positions of the genome with different coverage. For positions
415 covered by less than 1000 reads (95% of the genome) the expectation is 0 or 1
416 sequence mismatch (blue and orange lines). Positions with far greater numbers of
417 mismatches are likely due to sub-clonal mutations and technical bias.
418
419 **Figure 2 – figure supplement 1. RNA-seq mismatch rates for all trinuculeotides**
420 **in chromatin associated and nuclear RNAs. (a,b)** The 5' and 3 splicing motifs in
421 the human genome. **(c)** The RNA-seq mismatch frequencies for all single
422 nucleotides. **(d)** The RNA-seq mismatch rate to the reference genome for each
423 trinucleotide, normalized to the average mismatch rate across all trinucleotides. For
424 each trinucleotide, red shows the mismatch frequency at the first base, blue at the
425 second, and green at the third. Error bars are standard deviation across all samples.

426

427 **Figure 2 – figure supplement 2. RBP9 expression negatively correlates with**
428 **RNA-seq mismatch rates.** The mismatch frequency is shown across all cells lines.
429 **(a)** RPB9 mRNA expression is normalized by the median expression level of all
430 subunits. **(b)** RPB9 mRNA expression is normalized by RBP3 (POLR2C) expression.

431

432 **Figure 3 – figure supplement 1. Decreases in RPB9 and DST1 expression in**
433 **yeast results in more single base insertions in RNA-seq data.** For each RNA-seq
434 dataset, the number of inserts (+N) or deletions (-N) in the mpileup output (N is the
435 number o bases in the indel) were counted, and this number divided by the total
436 number of mapped reads in each sample. On the right are the same data but
437 zoomed in on each metric to better show the comparison between the two sets of
438 samples.

439

440 **Figure 3 – figure supplement 2. Mutations that affect transcription elongation**
441 **do not affect measured RNA-seq mismatch frequencies.** Two separate
442 experiments were performed with wild-type controls and mutants involved in
443 transcription elongation. Individual bars show the RNA-seq mismatch frequency of
444 biological replicates.

445

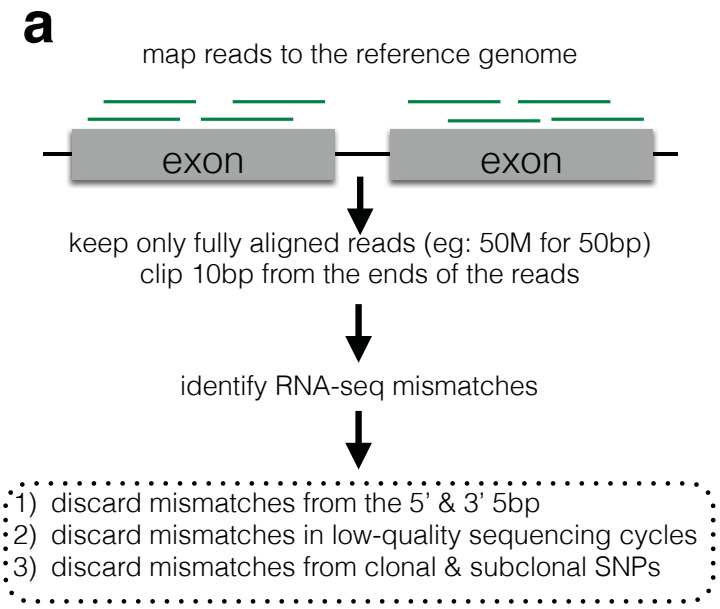
a
map reads to the reference genome
exon
exon
keep only fully aligned reads (eg: 50M for 50bp)
clip 10bp from the ends of the reads
identify RNA-seq mismatches
1) discard mismatches from the 5' & 3' 5bp
2) discard mismatches in low-quality sequencing cycles
3) discard mismatches from clonal & subclonal SNPs

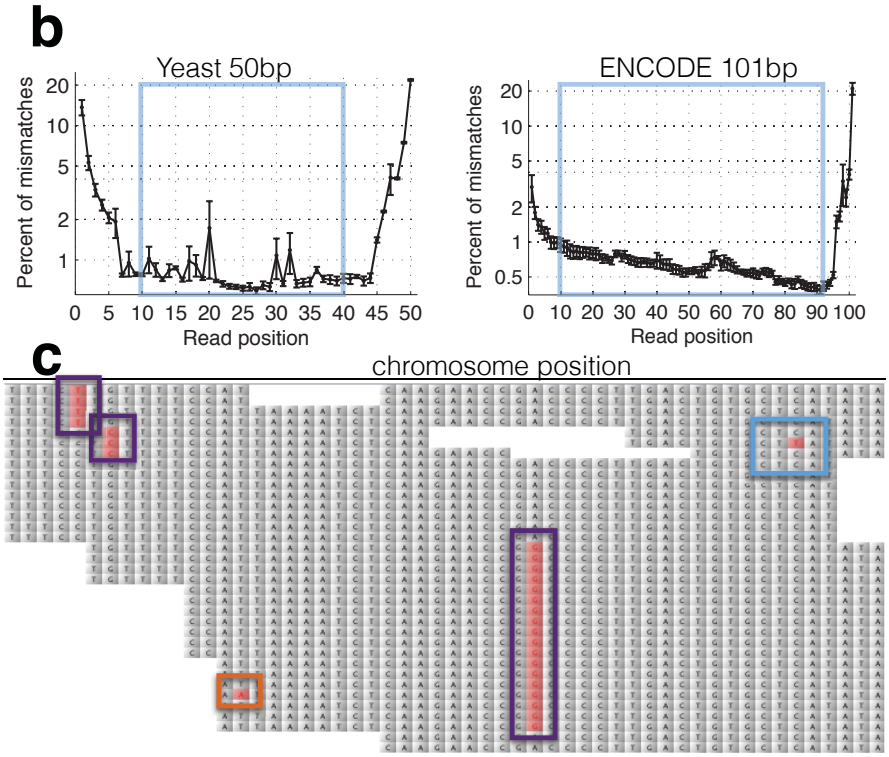
b
Yeast 50bp
ENCODE 101bp
Percent of mismatches
Read position
c
chromosome position

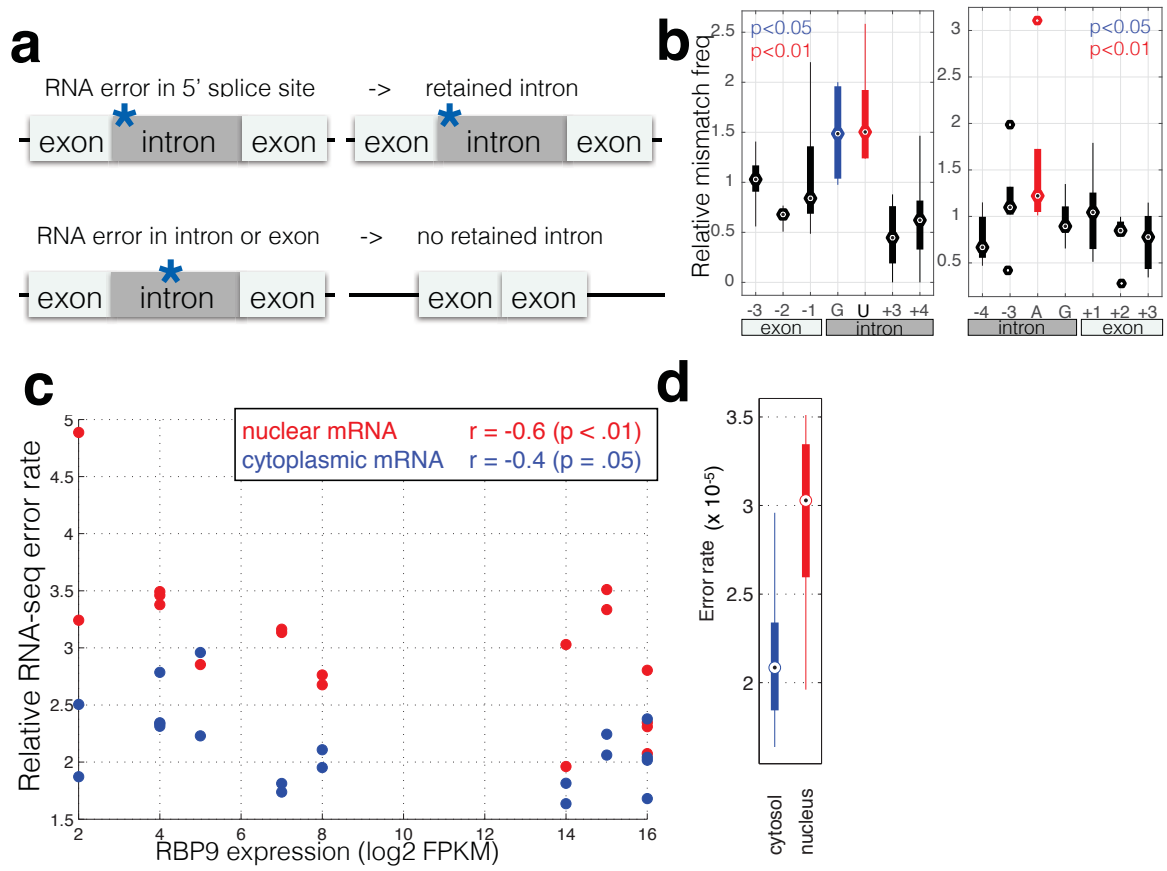
a
RNA error in 5' splice site
->
retained intron
exon
intron
exon
exon
intron
exon
RNA error in intron or exon
->
no retained intron
exon
intron
exon
exon
exon
b
Relative mismatch freq
p<0.05
p<0.01
-3 -2 -1 G U +3 +4
exon
intron
p<0.05
p<0.01
-4 -3 A G +1 +2 +3
intron
exon
c
nuclear mRNA r = -0.6 (p < .01)
cytoplasmic mRNA r = -0.4 (p = .05)
Relative RNA-seq error rate
RBP9 expression (log2 FPKM)
d
Error rate (x 10^-5)
cytosol
nucleus

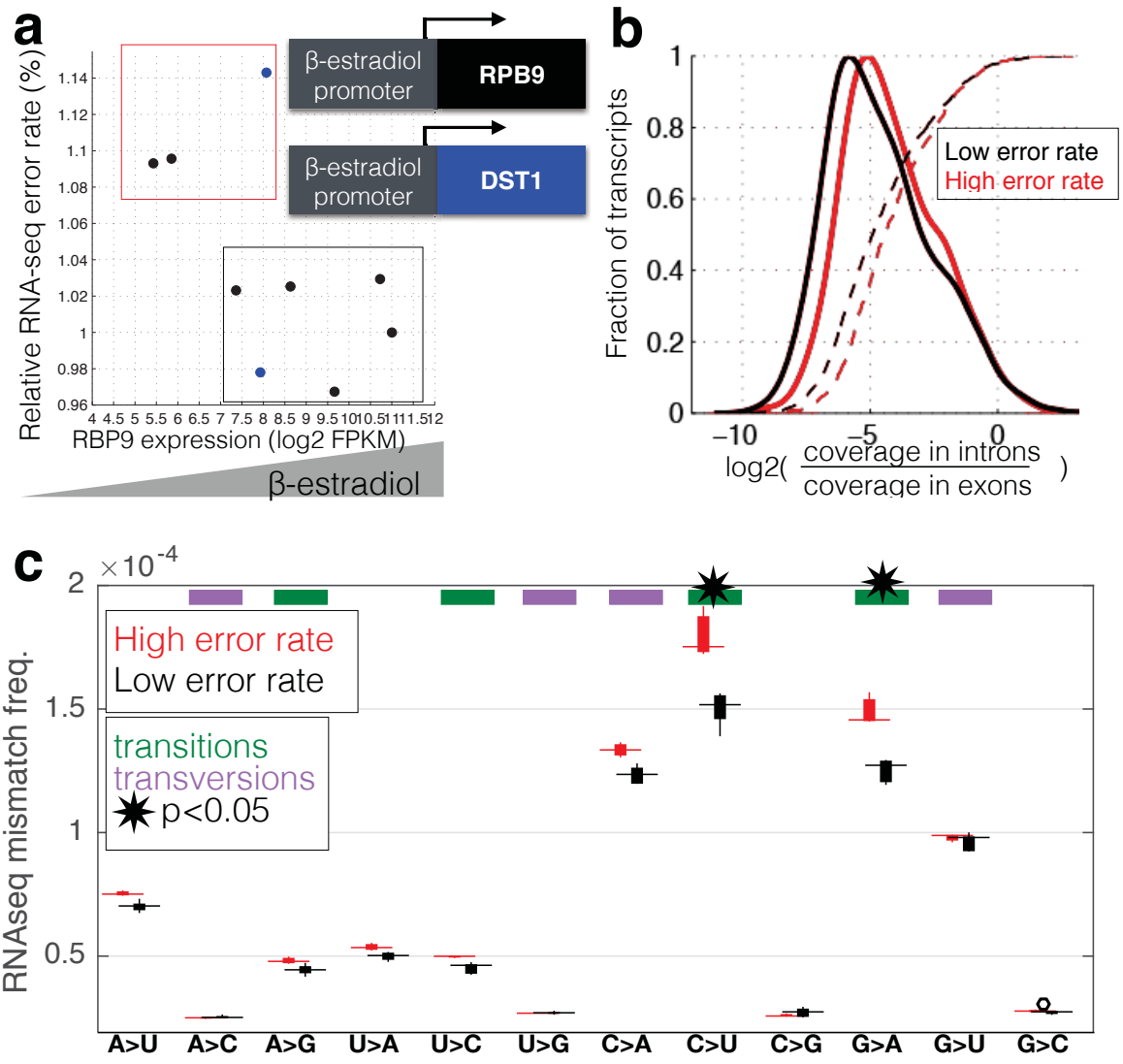
a
β-estradiol promoter
RPB9
β-estradiol promoter
DST1
Relative RNA-seq error rate (%)
RBP9 expression (log2 FPKM)
β-estradiol
b
Fraction of transcripts
Low error rate
High error rate
log2(coverage in introns / coverage in exons)
c
×10^-4
High error rate
Low error rate
transitions
transversions
p<0.05
RNAseq mismatch freq.
A>U
A>C
A>G
U>A
U>C
U>G
C>A
C>U
C>G
G>A
G>U
G>C

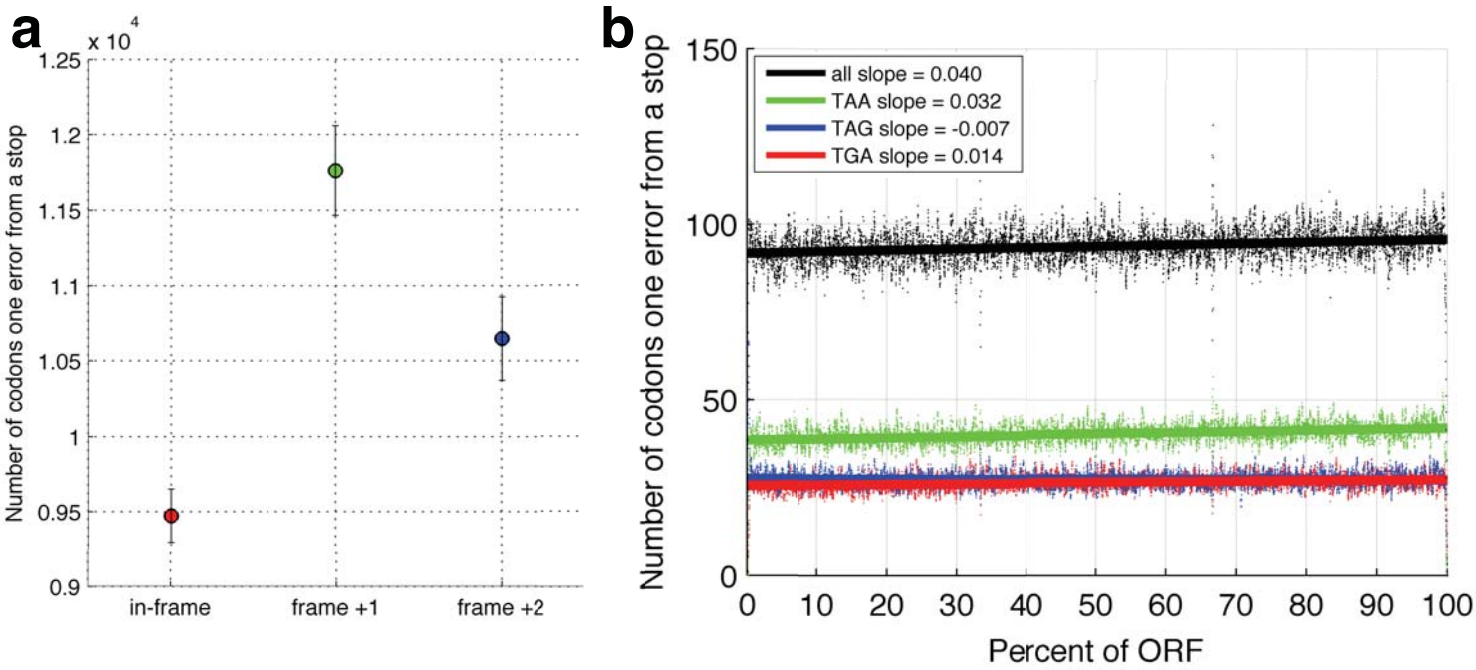
a
x 10^4
1.25
1.2
1.15
1.1
1.05
1
0.95
0.9
Number of codons one error from a stop
in-frame
frame +1
frame +2
b
all slope = 0.040
TAA slope = 0.032
TAG slope = -0.007
TGA slope = 0.014
150
100
50
0
Number of codons one error from a stop
0
10
20
30
40
50
60
70
80
90
100
Percent of ORF

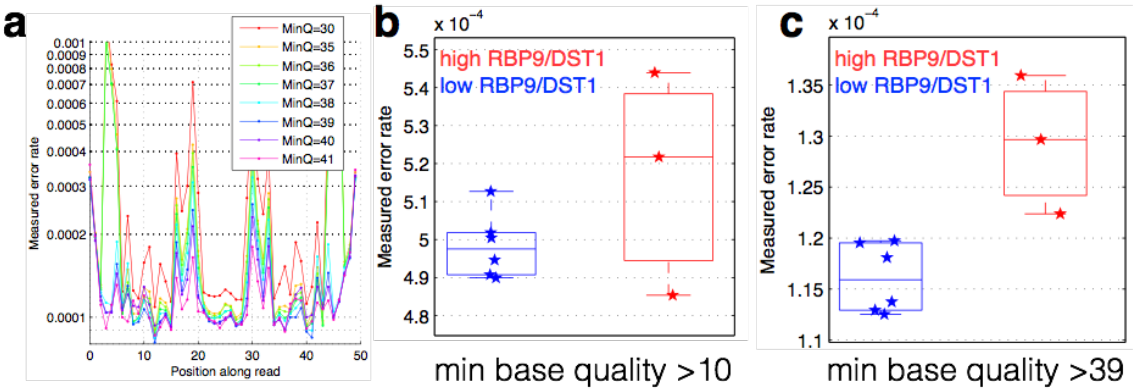

Figure 1 – figure supplement 1. Cycle-specific error rates and better differentiation of genetically determined error rates using base quality value cutoffs. Six yeast RNA-cDNA libraries were sequenced on the same lane in a HiSeq. **(a)** The average mismatch rate (across the six cDNA libraries) to the reference genome at each position was determined using different minimum base-quality thresholds using GATK ErrorRatePerCycle. Independent of the quality threshold, cycles at the ends, as well as some cycles in the middle, have high error rates. **(b)** The measured error rate for each sample using a minimum base quality of 10. **(c)** The measured error rate for each sample using a minimum base quality of 39.

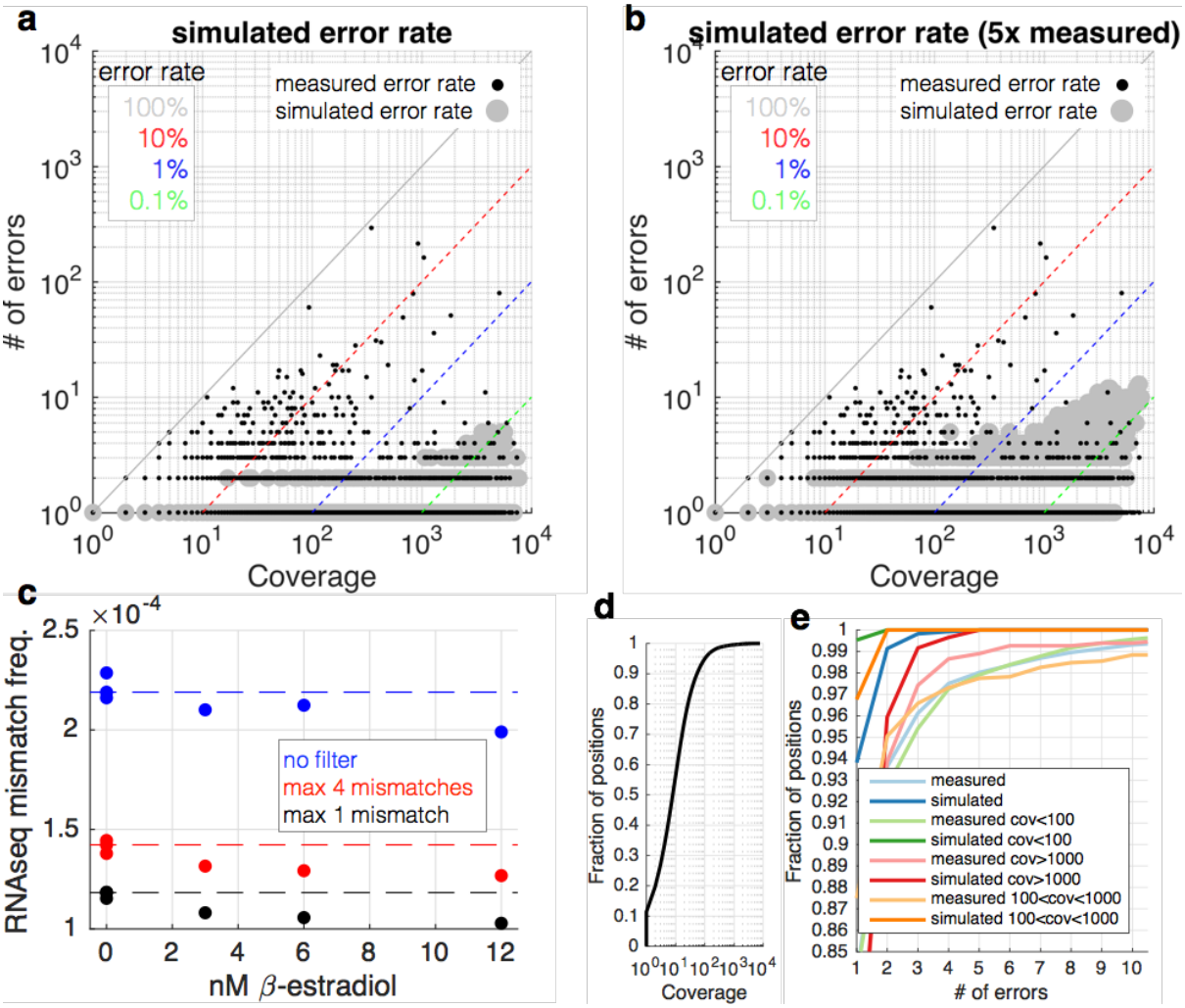

Figure 1 – figure supplement 2. RNA-seq data are enriched for mismatches to the reference genome that occur far more often than expected.

(a) At each coverage (x-axis), a point is shown if there is any positions in the genome with the observed number of errors (y-axis) (small black dots). The diagonal lines show mismatch frequencies of 100%, 10%, 1% and 0.1% — any point falling on these lines has the given mismatch frequency. With large grey circles are shown simulated data in which the same coverage as the yeast RNA-seq data are used, but with a mismatch frequency identical to the measured overall mismatch frequency of the yeast data. Locations in the graph in which a black point occurs but there is no grey point are locations in which there are more mismatches than expected by change. Note that at a coverage of less than 100, we expect to see no mismatches more than twice, and 0.5% of positions with 2 observances of identical mismatches. **(b)** Identical to (a) but with the simulated mismatch frequency 5x the observed. **(c)** Shown are measured mismatch frequencies for the yeast RPB9 and DST1 induction data at different B-estradiol concentrations, at different filters for the maximal allowed number of observed identical mismatches. The dashed lines show the average mismatch frequency for the 0nM condition. For all filters, low B-estradiol conditions have higher RNA-seq mismatch frequencies. **(d)** The coverage of the yeast RNA-seq data; ~95% of the genome is covered by less than 100 reads. **(e)** Shown are the fraction of positions in the genome (y-axis) with X errors (x-axis) for the yeast RNAseq data (cyan) and simulated data (blue). Also shown are the same data for positions of the genome with different coverage. For positions covered by less than 1000 reads (95% of the genome) the expectation is 0 or 1 sequence mismatch (blue and orange lines). Positions with far greater numbers of mismatches are likely due to sub-clonal mutations and technical bias.

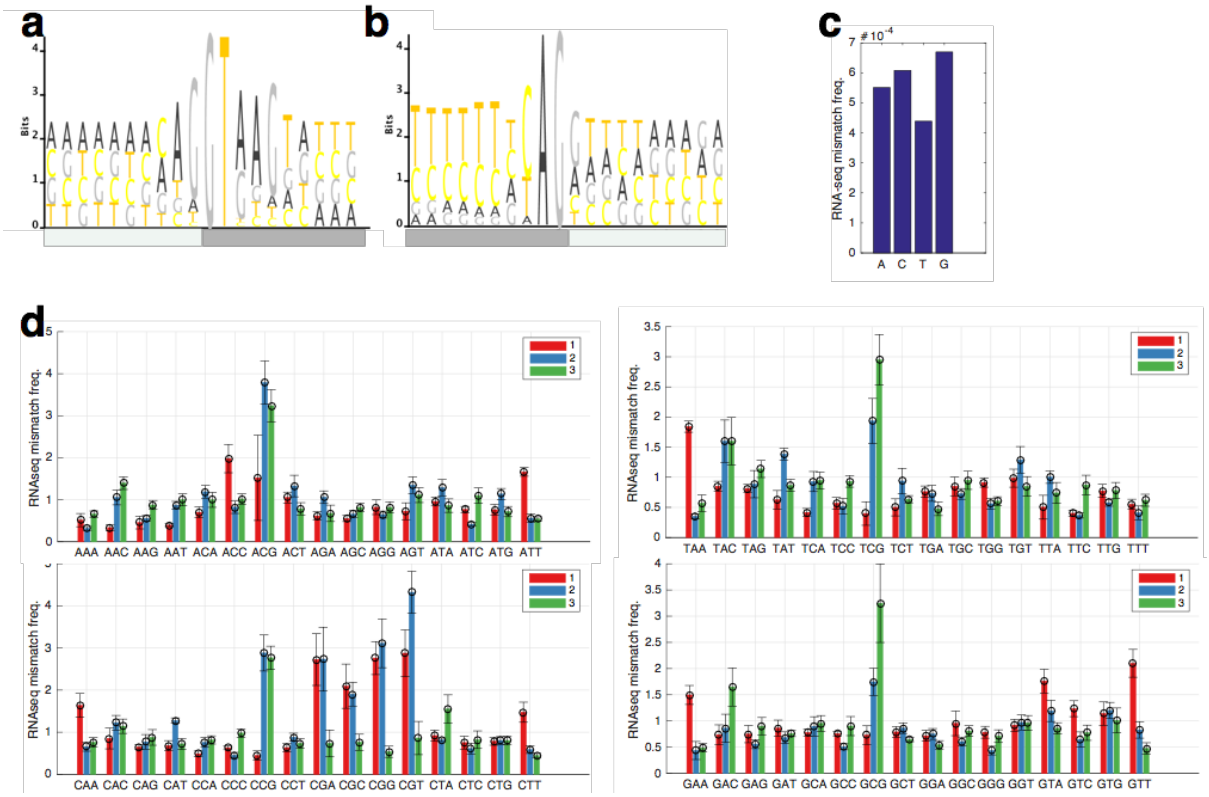

Figure 2 – figure supplement 1. RNA-seq mismatch rates for all trinucleotides in chromatin associated and nuclear RNAs. (a,b) The 5' and 3 splicing motifs in the human genome. **(c)** The RNA-seq mismatch frequencies for all single nucleotides. **(d)** The RNA-seq mismatch rate to the reference genome for each trinucleotide, normalized to the average mismatch rate across all trinucleotides. For each trinucleotide, red shows the mismatch frequency at the first base, blue at the second, and green at the third. Error bars are standard deviation across all samples.

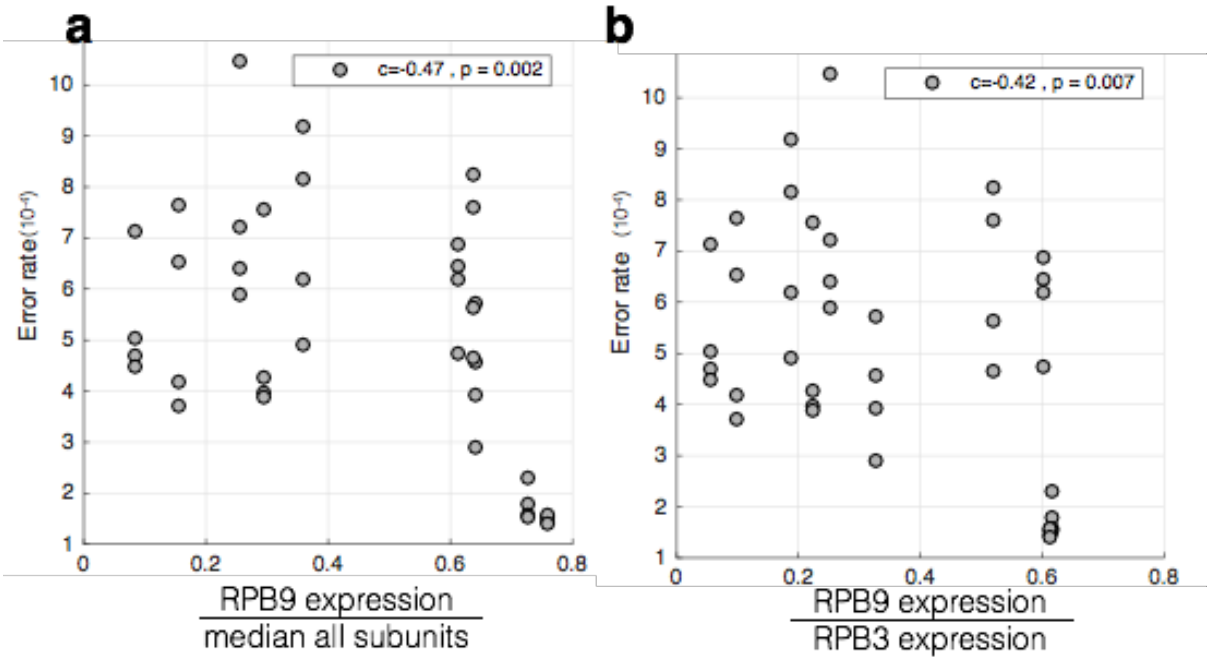

Figure 2 – figure supplement 2. RBP9 expression negatively correlates with RNA-seq mismatch rates. The mismatch frequency is shown across all cells lines. **(a)** RPB9 mRNA expression is normalized by the median expression level of all subunits. **(b)** RPB9 mRNA expression is normalized by RBP3 (POLR2C) expression.

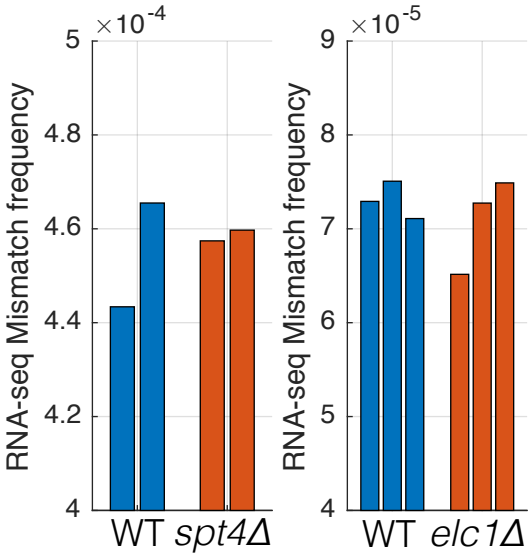

Figure 3 – figure supplement 1. Mutations that affect transcription elongation do not affect measured RNA-seq mismatch frequencies. Two separate experiments were performed with wild-type controls and mutants involved in transcription elongation. Individual bars show the RNA-seq mismatch frequency of biological replicates.